Collective band structure to high spin and shape coexistence in ^{76}Kr

R. B. Piercey, A. V. Ramayya, J. H. Hamilton, X. J. Sun, and Z. Z. Zhao
Department of Physics and Astronomy, Vanderbilt University, Nashville, Tennessee 37235

R. L. Robinson and H. J. Kim
Oak Ridge National Laboratory, Oak Ridge, Tennessee 37830

John C. Wells
Physics Department, Tennessee Technological University, Cookeville, Tennessee 38501
and Physics Division, Oak Ridge National Laboratory, Oak Ridge, Tennessee 37830
(Received 7 December 1981)

Excited states in ^{76}Kr have been investigated via the ^{66}Zn(^{12}C, $2n$) reaction at a beam energy of 39 MeV. Gamma-ray energies, intensities, spins, parities, and mean lives of excited states were extracted from measurements of the γ rays which were emitted in-beam. The energies of 25 excited levels were deduced from γ-γ coincidence data, and all but three of these levels are members of bandlike structures which persist to high spin. The Doppler shift attenuation method was used to extract the lifetimes of thirteen excited levels. The $E2$ strengths are highly collective. The positive parity yrast band to spin (12^+) has been observed with a forward bend at low spin, but with no backbending in the moment of inertia below 12^+. A positive parity band with even- and odd-spin members to (6^+) and (9^+) respectively, has been observed, and is interpreted as a $\Delta J=1$ quasigamma band. Negative-parity bands built on 5^- and (6^-) levels have been observed to spins of (13^-) and (12^-), respectively. Finally, the first excited 0^+ state and a 2^+ level built on it have been identified and are assigned to a near spherical configuration which coexists with the ground state that has an unusually large deformation.

NUCLEAR REACTIONS ^{66}Zn(^{12}C,$2n$) $E=39$ MeV; measured E_γ, I_γ, $\gamma(\theta)$, DCO, DSAM; deduced ^{76}Kr levels, J, π, $B(E2)$, δ, and γ branching.

I. INTRODUCTION

The nuclei in the mass region $A\approx 60-80$ have become, in recent years, a rich testing ground for both nuclear models[1-4] and new experimental techniques.[5,6] The nuclei are only a few nucleons away from the N, $Z=28$, 50 closed shells; nonetheless highly collective structures have been observed to high spin [e.g., up to tentative 20^+ in ^{74}Kr (Ref. 7)]. Shape coexistence with bands of levels built on quite different deformations has been reported in this mass region.[1] Gamma vibrational-like bands[8] analogous to those in very deformed nuclei have been seen up to spin 9^+. Quasiparticle degrees of freedom, which are responsible for "backbending" of the moment of inertia in well deformed rare earth nuclei, also are established in this region.[4] Surprisingly large collectivity in these few nucleon systems, particularly ^{72}Se, is indicated by the $B(E2)$ values. However, in ^{70,72}Ge the $B(E2)$ values are not nearly as collective and well developed bands built on the excited 0^+ states that would indicate large deformations are not observed.[1] Prior to this study the 2^+, 4^+, and 6^+ yrast levels in ^{76}Kr were known and the 8^+ and 10^+ yrast levels were suggested.[9] The study of ^{76}Kr reported here has added much information about the band structure and shape coexistence in nuclei in the 60–80 mass region as well as the subshell closure at $N=40$. The 0_2^+ state has been identified and is the lowest in this mass region, except for ^{72}Ge (also $N=40$) where it is the first excited state. The 0_2^+ state in ^{76}Kr is interpreted as a near spherical configuration that exists with a ground state with unusually large deformation. These data provide a clearer picture of shape coexistence in this mass region.

II. EXPERIMENTAL PROCEDURES

The gamma-ray spectroscopy studies described in this paper were performed at the Oak Ridge National Laboratory 6.5-MV tandem Van de Graaff facility. An enriched ^{66}Zn target was bombarded with ^{12}C ions at 39 MeV. A singles gamma-ray spectrum observed with a Ge(Li) spectrometer is shown in Fig. 1. The lines in ^{76}Kr, which result from the (^{12}C,2n) reaction, are among the strongest observed. Other strong channels are ^{76}Br + pn and ^{76}Se + 2p channels. Such singles spectra were taken at 0°, 55°, and 90° with respect to the beam direction at a distance of 15 cm from the target. A monitor detector was kept at −90° for normalization purposes. Gamma-gamma coincidence data were taken with one Ge(Li) detector at 0° and another at 90° with a time resolution of $2\tau \cong 50$ ns. The coincidence data were stored in a 1024×1024 matrix for off-line analysis. Energy and efficiency calibrations were performed with calibrated RaE sources placed at the target position. This method was also used to determine the decentering effects of the target in the angular distribution measurements.

III. ANALYSIS AND RESULTS

Several coincidence spectra are shown in Figs. 2 and 3 to illustrate the quality of the gamma-gamma coincidence data. All the levels shown in Fig. 4 have been placed on the basis of their coincidence relations. There are a few additional lines in the 424-keV gate (see Fig. 2). However, since these

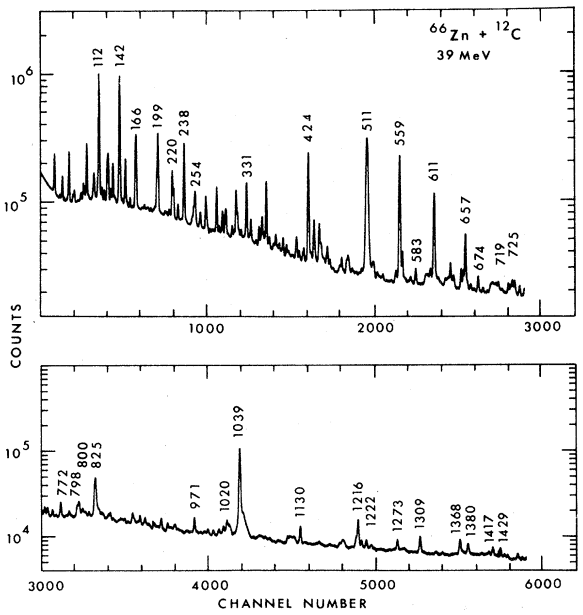

FIG. 1. Singles γ-ray spectrum observed in-beam with ^{12}C on ^{66}Zn at 39 MeV.

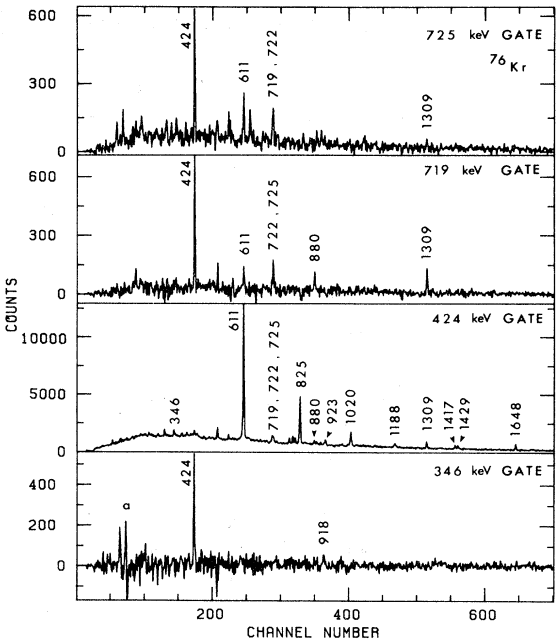

FIG. 2. Representative coincidence spectra with the gates as shown. The spectra are corrected for background coincidences. The peaks marked "a" represent oscillations in the back-scattered region because of improper corrections for the background coincidences.

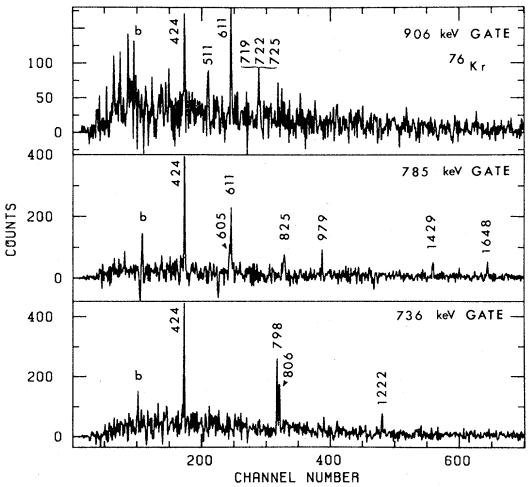

FIG. 3. Representative coincidence spectra with the gates as shown. The spectra are corrected for background coincidences. The peaks marked "b" represent oscillations in the back-scattered region because of improper corrections for the background coincidences.

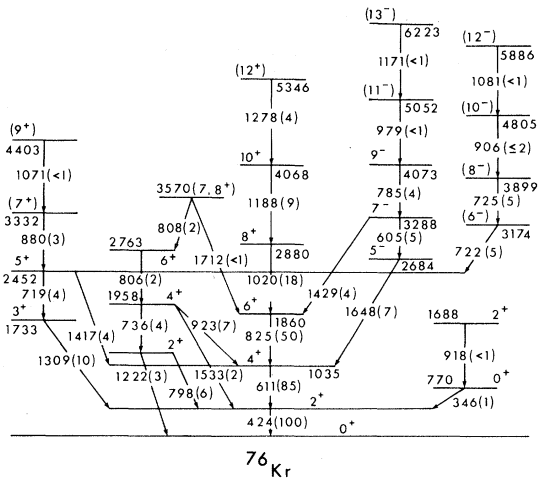

FIG. 4. Level scheme of ^{76}Kr.

lines are not present in gates on any other transitions in ^{76}Kr and are quite weak, they have not been placed in the decay scheme. Evidence for the placement of the levels at 770 and 1688 keV is indicated in the 424- and 346-keV coincidence spectra. The placement of these levels has been confirmed by our decay studies[10] of mass separated ^{76}Rb.

The gamma-ray relative intensities and angular distribution coefficients were extracted for many of the transitions in ^{76}Kr from the angular distribution measurements by fitting the normalized singles counting rates, $W(\theta)$, at 0, 55, and 90 deg to the well-known fourth-order Legendre polynomial expansion:

$$W(\theta)=A_0[1+Q_2\alpha_2 a_2^{\max}P_2(\cos\theta) + Q_4\alpha_4 a_4^{\max}P_4(\cos\theta)] .$$

The Q_2 and Q_4's are corrections which account for the finite solid angle of the detector and can be calculated from the known detector characteristics. The respective ranges of Q_2 and Q_4 were 0.974—0.975 and 0.917—0.918. The α_2's and α_4's are the parameters which describe the degree to which the initial state is aligned and must, in principle, also be determined from the fit to the experimental data; however, it is usually sufficient to know the products $a_2=\alpha_2 a_2^{\max}$ and $a_4=\alpha_4 a_4^{\max}$ in determining the change in spin which accompanies the transition. Measured values of the α_2 parameter range from $\sim$0.45 for the 424-keV level to $\sim$1.00 for levels higher in energy. A value of 1.00 for α_2 corresponds to complete $m_z=0$, alignment of the initial state. In cases where ambiguity remains, α_2 and α_4 can be related by assuming a Gaussian distribution of magnetic substates in the initial state and thereby an additional constraint may be introduced. Relative intensities for the gamma rays whose angular distributions could be extracted from the singles data are calculated by dividing the intensity, A_0, of each gamma ray by the detector efficiency and then normalizing them to A_0 (424 keV) $=100$. The relative intensities are given in Fig. 4. The errors are generally of the order of 5% for I_γ. In several cases, however, statistics are too poor or the spectra are too complex in the singles data to allow determination of the intensity in this way. In such cases, the intensities must be extracted from the coincidence data and corrected for the assumed angular distribution. In most of these cases, only an upper limit could be determined as shown in Fig. 4. The angular distribution coefficients, a_2 and a_4, the alignment parameters α_2 and the δ-mixing parameters, which could be determined in this experiment are presented in Table I.

States which are placed on the basis of our coincidence data must decay with mean lives $\tau \lesssim 100$ ns. For this reason it is assumed that no multipoles of order higher than $E2$ or $M1$ may dominate in the transitions that we have studied. By assuming that $E1$, $E2$, and $M1$ multipoles may be observed, then the mixing ratio $\langle||L+1||\rangle/\langle||L||\rangle$, where L is the lowest allowed multipole, can be extracted from the angular distribution data. In the actual analysis the transition is assumed to be pure quadrupole when the spin difference is equal to 2 and to have quadrupole and dipole components when the spin difference is equal to 0 or 1. In Table I, δ values are given for those spin sequences which are consistent with the angular distribution measurements. The phase convention is that of Biedenharn and Rose.[11]

The directional correlation from oriented nuclei (DCO ratio) was extracted from the γ-γ coincidence data for many of the transitions in ^{76}Kr. The experimental DCO ratio is defined as $R=W(90°, 0°)/W(0°,90°)$, where the two angles refer to the first and second members of the γ-ray cascade for the respective choice of angles. The DCO ratios were calculated by using the δ and α_2 values which were extracted from the angular distribution measurements. Table II compares the experimental values to the theoretical ratios[12] calculated for the spin sequences which are consistent with the $\gamma(\theta)$ measurements (see Table I). It is clear from Table II that the DCO ratio may, in many cases, be used to eliminate some of the spin sequences which were consistent with the $\gamma(\theta)$ measurement. Gamma-ray energies were determined by using the known

TABLE I. Angular distribution results for ^{76}Kr.

E_{level}	E_γ	a_2	a_4	J^π_{final}	$J^\pi_{initial}$	δ^a $\frac{\langle\|\|L+1\|\|\rangle}{\langle\|\|L\|\|\rangle}$	α_2
423.9	423.9	0.31(1)	−0.14(1)	0^+	2^+		0.45(3)
769.6	345.7	0.06(5)	−0.06(7)	2^+	0^+		
					2	−0.29(5)	≥0.2
1034.7	610.8	0.36(1)	−0.15(1)	2^+	2	2.36(8)	0.77(3)
					4^+		0.73(3)
1221.5	1221.5	0.52(4)	−0.12(5)	0^+	2^+		0.58(5)
1732.6	1308.7	0.24(3)	−0.02(2)	2^+	2	0.00(2)	0.6(3)
					3	0.38(4)	0.6(1)
1859.5	824.8	0.30(2)	−0.14(2)	4^+	4	1.2(2)	0.77(10)
					6^+		0.75(10)
1957.6	736.0	0.28(3)	−0.18(4)	2^+	2	3.0(2)	0.81(10)
					4^+		0.65(10)
	922.6	−0.19(2)	−0.22(3)	4^+	4	23(14)	0.73(5)
					4	−0.84(5)	0.97(6)
2451.3	1417.2	0.34(4)	0.20(5)	4^+	3	−2.0(6)	0.99(5)
					5	4(2)	0.72(2)
2683.5	1647.8	−0.21(3)	−0.07(5)	4^+	3	0.05(3)	~0.85[b]
					5	0.04(3)	~0.85[b]
2879.6	1020.1	0.39(2)	−0.13(2)	6^+	6	0.74(4)	0.85(10)
					8^+		0.90(10)
3288.1	605.1	0.38(5)	−0.29(7)	5^-	5	1.1(2)	0.96(12)
					7^-		1.00(12)
	1428.6	−0.31(4)	0.05(5)	6^+	5	0.08(3)	~0.90[b]
					7	0.00(4)	~1.00[b]
4068.0	1188.4	0.30(2)	−0.16(3)	8^+	8	0.85(6)	0.86(10)
					10^+		0.82(10)

[a]The $\Delta I=2$ transitions are assumed to be pure quadrupole radiation.
[b]Estimated from nearby levels.

gamma-ray energies of a Ra*E* source. The relative efficiency of the detector system was determined by comparing the measured areas of gamma rays from the same Ra*E* source to their known relative intensities. In Table III the measured transition energies, deduced level energies, and the spin/parity assignments are given. The arguments on which the spin/parity assignments are based are also summarized in Table III.

Mean lifetimes of levels from the 0° singles and coincidence spectra were extracted by the Doppler shift attenuation method (DSAM). Coincidence spectra produced by gating on γ rays below and in some cases above the level of interest were analyzed. In some cases the sum spectra in coincidence with two or three transitions were used. The program DOPCO (Ref. 13) was used to extract the lifetimes. A preliminary report of these results has been given.[14] By using stopping powers and the initial velocity of the recoiling nuclei, the Doppler shifted line shape can be calculated for different lifetimes. Thus, the only unknown value in the calculations is the lifetime of the level. Computed spectra are fitted to experimental spectra and the lifetimes extracted from the fits by a χ^2 minimization procedure. The total stopping power is considered to arise, from the electronic interactions of the ion in the stopping material and the nuclear-nuclear interactions. One therefore writes the total stopping power in terms of the reduced, dimensionless variables ρ and ϵ as

$$\left.\frac{d\epsilon}{d\rho}\right|_t=\left.\frac{d\epsilon}{d\rho}\right|_n+\left.\frac{d\epsilon}{d\rho}\right|_e ,$$

where

$$\epsilon=E(aA_T)/Z_PZ_Te^2(A_P+A_T) ,$$

$$\rho=\chi(NA_T\cdot A_P4\pi a^2)/(A_P+A_T)^2 ,$$

TABLE II. DCO measurements in ^{76}Kr.

$E\gamma_1$ (keV)	$E\gamma_2$ (keV)	R_{exp}	Spin sequence	δ	α_2	R_{cal}
611	424	1.00(2)	2→2→0	2.36(8)	0.77(3)	0.37(3)
			4→2→0	*E*2		1.00
825	611	1.02(4)	4→4→2	1.2(2)	0.77(3)	0.88(7)
			6→4→2	*E*2		1.00
825	424	1.03(3)	4→4(→)2→0	1.2(2)	0.77(3)	0.88(7)
			6→4(→)2→0	*E*2		1.00
1020	825	1.01(8)	6→6→4	0.74(4)	0.85(10)	0.89(2)
			8→6→4	*E*2		1.00
1020	424	0.99(5)	6→6(→)4(→)2→0	0.74(4)	0.85(6)	0.89(2)
			8→6(→)4(→)2→0	*E*2		1.00
346	424	1.3(3)	2→2→0	−0.29(5)	0.34	1.40(10)
			0→2→0	*E*2		1.00
1309	424	0.81(7)	2→2→0	0.00(2)	0.6(3)	0.99(5)
			3→2→0	0.38(4)	0.6(1)	1.08(9)
798	424	0.74(10)	2→2→0	0.2(1)[a]	0.58(5)[b]	
923	424	0.82(23)	4→4(→)2→0	1.0(5)[a]	0.73(5)	
			4→4(→)2→0	−0.8(3)	0.97(6)	4(2)
1417	611	0.89(18)	3→4→2	−2.0(6)	0.99(5)	1.1(2)
			5→4→2	4(2)	0.72(3)	0.8(2)

[a]Determined from the measured DCO ratio.
[b]From the 1221 keV transition.

and

$$a = a_0 0.8853 (Z_P^{2/3} + Z_T^{2/3})^{-1/2} .$$

In these formulas $A_P(A_T)$ and $Z_P(Z_T)$ are the atomic mass and atomic number of the projectile (target); a_0 is the Bohr radius; N is the density in atoms per cm^3; χ is the distance in cm; and E is the energy. For these calculations, we have taken for the nuclear part of the total stopping, $d\epsilon/d\rho\,|_n$, the Bohr formula[15] which results from the well known Rutherford scattering process. In reduced variables it can be written simply as

$$\left.\frac{d\epsilon}{d\rho}\right|_n = \frac{1}{2\epsilon}\ln(2\epsilon) .$$

Kalbitzer *et al.*[15] have shown that this formula gives values which are too low by as much as 50% for $\epsilon \approx 1$. This is the point at which the electronic and nuclear terms in the expression for the total stopping power are approximately equal, and the total stopping power has a minimum.

The depth of this minimum may significantly effect the quality of the fit in the region where the shifted and unshifted parts of the Doppler line shape merge, but it should not produce significant errors in the measured lifetimes. The Bohr expression was chosen since it is somewhat simpler and, in general, is better known than the formula of Kalbitzer *et al.*[15]

The extracted lifetimes are more sensitive to the electronic part of the total stopping power because it is much larger than the nuclear part over most of the range of velocities which are considered in these calculations. Attempts to calculate the electronic stopping powers for arbitrary projectile-target systems have in general been unsuccessful. However, extensive tabulations of experimental data and numerical interpolations of the data for a large number of projectile-target combinations do exist.[16,17] In our calculation we took the electronic stopping power for ^{76}Kr in ^{66}Zn from the tables of Northcliff and Schilling.[16] These tables are known to have large errors for particular targets in the form of a Z_2-dependent oscillation.[17] We therefore scaled the data as suggested by Ward *et al.*[18] by taking the values of Ziegler and Chu[17] for α particles stopping in ^{66}Zn. The scaled values are given by

TABLE III. Spin/parity assignment in ^{76}Kr.

E_{level}	E^*_γ	$\gamma^{(\theta)}_{DCO}$	Decay mode	Expected from systematics	Previous assignments	Adopted J^π	δ
423.9	423.9	2^+	$1,2^+$	2^+	2^+	2^+	
769.6	345.7	$0^+,2$		0^+		0^+	
1034.7	610.8	4^+		4^+	4^+	4^+	
1221.5	1221.5	2^+	$1,2^+$	2^+		2^+	0.2(1)
	797.6						
1688	918		$1,2^+$	2^+	(2^+)		
1732.6	1308.7	2,3		3^+		3^+	0.38(4)
1859.5	824.8	6^+		6^+		6^+	
1957.6	736.0	2,4	$2^+,3,4^+$				
	922.6	4		4^+		4^+	1.0(5)
	1532.9						
2451.8	1417.2	(3),5		5^+		(5^+)	4(2)
2683.5	1647.8	3,5		5^-		5^-	0.04(3)
2762.8	805.6			6^+		6^+	
2879.6	1020.1	8^+		8^+		8^+	
3174.1	722.3			6^-		(6^-)	
3288.1	605.1	$5,7^-$		7^-		7^-	
	1428.6	5,7					
3331.7	879.9			7^+		(7^+)	
3570.5	807.7			$7,8^+$		$(7,8^+)$	
	1712						
3899.2	725.2			8^-		(8^-)	
4068.0	1188.4	$8,10^+$		10^+		(10^+)	
4073.0	784.7			9^-		(9^-)	
4403	1071			9^+		(9^+)	
4805	906			10^-		(10^-)	
5052	979			11^-		(11^-)	
5346.0	1278.0			12^+		(12^+)	
5886	1081			12^-		(12^-)	
6223	1171			13^-		(13^-)	

$$\frac{dE}{dX_e}=\frac{\left(\frac{dE}{dX}\right)^{N-S}\left(\frac{dE}{dX_\alpha}\right)^{Z-C}}{\left(\frac{dE}{dX_\alpha}\right)^{N-S}}\,.$$

The magnitude of the scaling is about 17% and the resulting electronic stopping powers should be accurate to less than 10%.

As the recoiling nucleus slows to very low velocity, multiple nuclear scattering becomes important. The effect of multiple scattering is to reduce the component of velocity in the initial recoil direction and is calculated approximately by the Blaugrund formalism.[19] These corrections along with others which include the slowing of the projectile in the target, angular distribution of the γ rays, detector solid angles, and feeding times from higher states are included in the extraction of the lifetimes. Some lifetimes are considered composite as indicated in Table IV, because we assumed that the nondiscrete side feeders have very short lifetimes. Indeed for these transitions the side feeders may have long lifetimes based on the case of the $9^-\rightarrow 7^-$ transition where we demonstrated that the side feeders have measurable lifetimes.

Lifetimes of the highest two levels in the ground band were extracted from the singles spectrum observed at 0° and others were from coincidence spectra. As seen in Fig. 5, the highest observed yrast lines exhibit rapidly increasing Doppler shifts from which lifetimes are easily extracted. Coincidence spectra can be used to eliminate the contributions

TABLE IV. Level or composite-level plus feeding-mean-lifetimes and transition strengths are given.

E_{level} (keV)	E_γ (keV)	I_i-I_f	τ_{mean} (ps) (error)	$B(E2)/B(E2)_{sp}$
424	424	2^+-0^+	53(7)[c]	59(7)
1035	611	4^+-2^+	5.0(20)	76^{33d}_{18}
1860	825	6^+-4^+	1.25(12)	89(8)
2880	1020	8^+-6^+	0.30(3)	129(13)
4068	1188	10^+-8^+	0.14(2)	129(19)
5346	1278	(12^+)-10^+	0.24(5)[a]	52(11)[a]
6223	1171	(13^-)-(11^-)	0.34(8)[a]	57(14)[a]
5052	979	(11^-)-9^-	0.18(7)	264^{242}_{74}
4073	785	9^--7^-	0.51(11)[a]	281^{77a}_{50}
			0.16(6)[b]	895^{538}_{244}
3288	1429	7^--6^+	0.37(6)	
	605	7^--5^-		863^{170}_{121}
4403	1071	(9^+)-(7^+)	0.42(10)[a]	72^{23a}_{14}
3332	880	(7^+)-5^+	1.03(3)[a]	79(3)[a]
2452	1417	5^+-4^+	1.1(4)[a]	3.4^{8a}_{5}
	719	5^+-3^+		101^{22a}_{16}
1953	736	4_2^+-2_2^+	1.3(4)[a]	47^{21a}_{11}
	923	$4_2^+ \rightarrow 4^+$		27^{10a}_{6}
	1533	$4_2^+ \rightarrow 2^+$		0.6(2)[a]

[a]Composite lifetime and composite $B(E2)$ compared to a single particle.
[b]Lifetime obtained from gating above the transition of interest.
[c]Nolte *et al.* (Ref. 9).
[d]Based on an average=6.6 ps from this paper and Nolte *et al.* (Ref. 9).

from side feeding transitions with unknown lifetimes and from the γ rays which are not in coincidence with the gating transition. However, the statistical accuracy in the coincidence spectra is too poor for the weakest transitions to yield meaningful lifetimes. Also by comparing the coincidence spectra from gates above and below the transition of interest, we have obtained some information on the

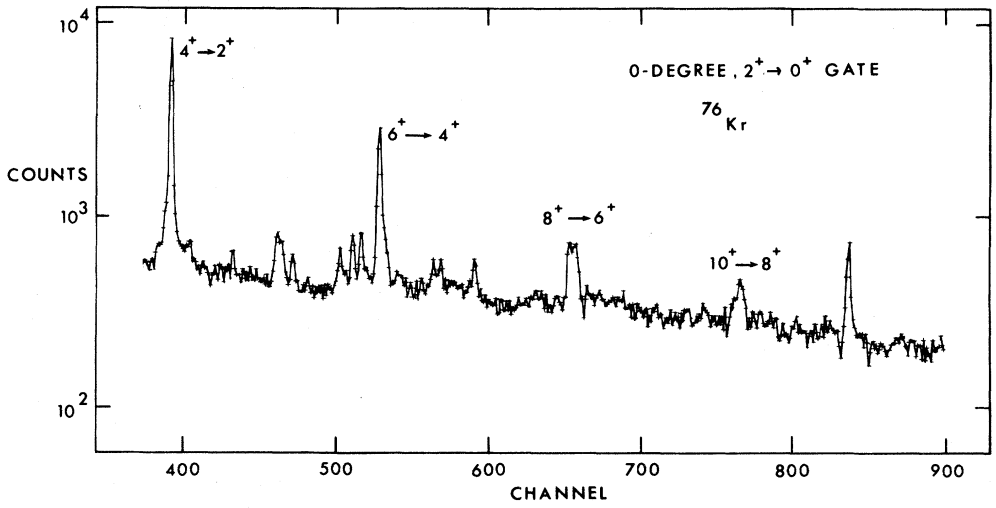

FIG. 5. Doppler shifts of the yrast lines observed with a detector at 0°.

lifetimes of the unobserved side feeding.

The lifetimes of the ground band and other levels are shown in Table IV and an example of one of the fits is shown in Fig. 6. Since feeding times of transitions into the 12^+ state are not known, only a composite feeding-decay time is obtained. This level's lifetime is certainly shorter than the composite one.

By gating on transitions above and below the $6^+ \rightarrow 4^+$ transition, the contribution of the lifetimes of the side feeders to the composite lifetime was shown to be negligible for this state (the extracted 6^+ lifetime was the same in both gates). That is the lifetimes of the side feeders are short compared to the lifetime of the $6^+ \rightarrow 4^+$ transition. Similarly, equal lifetimes from gates above and below the 8^+-6^+ transitions were found but with somewhat larger errors ($\sim 15\%$). On the other hand, feeding times were shown to be important for the 9^--7^- transition. The unobserved side feeders which compose over 75% of the feeding to the 9^- level have surprisingly long lifetimes as shown by the quite different lifetimes extracted when gating above (correcting for the measured composite lifetimes of the gating transition) and below (Table IV).

IV. DISCUSSION

As seen in Fig. 4, it is striking that almost all the observed levels in ^{76}Kr can be classified into bands. Judged from the crossing between bands only at low spins, they appear very pure. Bands similar to these have been identified in nearby nuclei.[8,20] The even- and odd-spin $\Delta J = 2$ cascades based on the 2^+ level at 1222 keV and the 3^+ at 1733 keV, respectively, form a quasigamma type band to (9^+). The ground-state band is observed to (12^+). A $\Delta J = 2$, odd-parity band with odd spin members and even spin members have been identified to (13^-) and tentatively (12^-), respectively. In addition, the first excited 0^+ state has been identified at 770 keV, and a state at 1688 keV that feeds it has been assigned 2^+ based on our work and recent decay studies.[10]

Plots of moments of inertia ($2\mathcal{I}/\hbar^2$) versus the square of the rotational energy $(\hbar\omega)^2$ in the ground-state bands of the even-even krypton isotopes[7,20,21] are shown in Fig. 7. The plots exhibit varied effective behavior. It is clear that between spin 2 and 4 the slope of the plot increases as the isotopes become more neutron deficient. Figure 8 shows the yrast states of the Kr isotopes plotted in a different way. The differences in successive gamma-ray energies, $\Delta^2 E$, are plotted versus the spin. Such a plot is not only model independent and directly related to the experimental gamma-ray energies but is also very sensitive to any change in structure in the yrast bands. In Fig. 8 the curves of $\Delta^2 E$ versus spin for

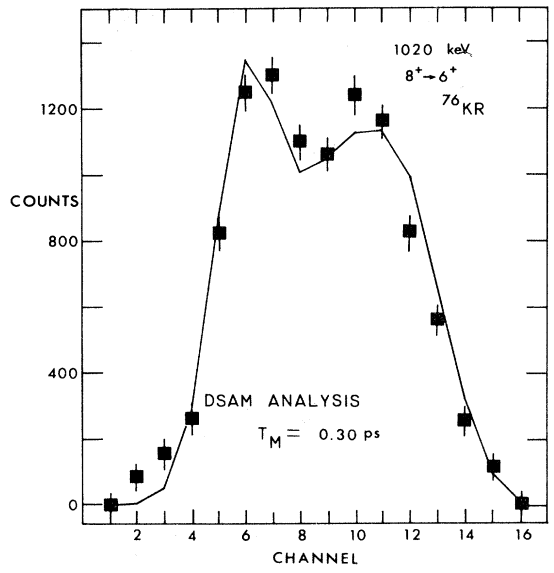

FIG. 6. DSAM line shape analysis of the $8^+ \rightarrow 6^+$, 1020 keV transition in ^{76}Kr.

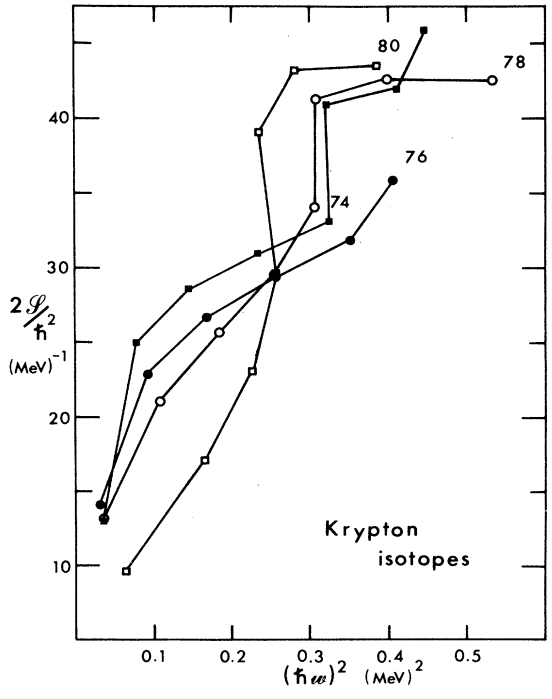

FIG. 7. Plots of moments of inertia ($2\mathcal{I}/\hbar^2$) vs the square of the rotational energy $(\hbar\omega)^2$ in the ground state bands of the even-even krypton isotopes.

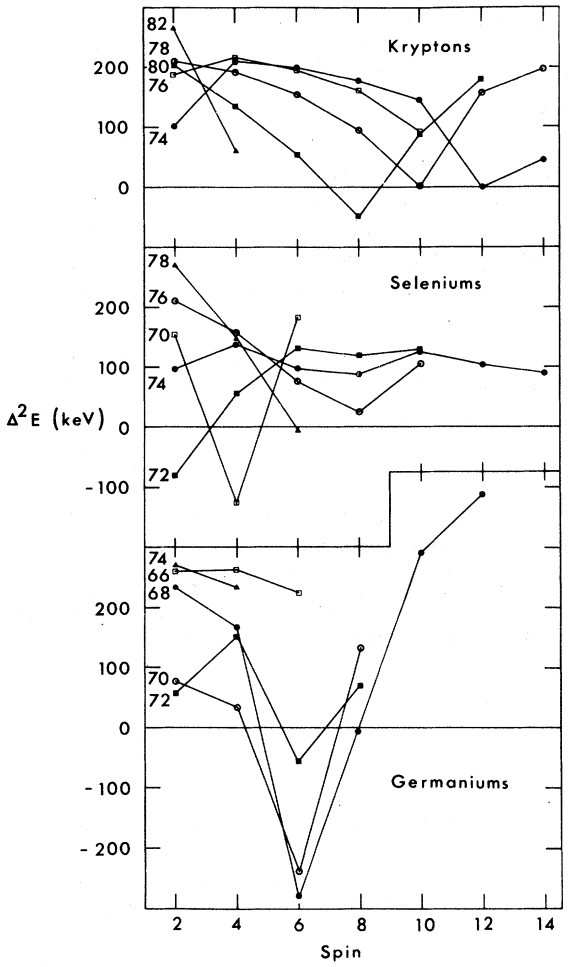

FIG. 8. The curves of successive gamma-ray energies (Δ^2E) of yrast transitions vs intermediate level spin for even-even krypton, selenium, and germanium isotopes.

yrast transitions in the even-even krypton isotopes are similar between spins of 4 and 8. Backbending of $\mathcal{I}$ is now seen clearly at spin 8 as a negative point on the curve for ^{80}Kr with sharp minima in the curves for ^{74,78}Kr at spins 12 and 10, respectively. These minima in the ^{74,78,80}Kr are interpreted as the crossing of the ground band by a band built on a $(g_{9/2})^2$ proton configuration.[1,21,25] It crosses at higher spin because the two-quasiparticle energies are nearly constant while the ground-band energies decrease because of larger deformation as N decreases.

At low spin, $2\rightarrow4$, the curves indicate a further anomaly which is not apparent in ^{80}Kr but which grows increasingly stronger as the nucleus becomes more neutron deficient. The anomalously low points at spin 2 for ^{74,76}Kr indicate a compression of the $4^+\rightarrow2^+$ and higher transition energies compared to the $2^+\rightarrow0^+$ energy. Figure 9 shows the low energy level systematics of some of the even-even krypton isotopes and indicates, at least for the 0_2^+ states which are known, that the strength of the low spin anomaly is correlated with the lowering of the 0_2^+ state. The Δ^2E plot shown in Fig. 8 for selenium and germanium nuclei show a similar correlation at low spin. In ^{72,74}Se this low spin anomaly was interpreted in terms of a shape coexistence model,[1,8,22,23] where the excited 0_2^+ level is the bandhead for a configuration with much larger deformation than the ground state. There is mixing of the 2^+ near spherical and deformed states. In a recent Letter[24] we have pointed out that the low spin anomalies in ^{74,76}Kr can be understood in a shape coexistence picture where now the ground state is deformed and the 0_2^+ state is near spherical. Evidence for such includes the much larger $2\text{-}0_2^+$ energy compared to the $2_1\text{-}0_1^+$ energy and the rotational behavior of the yrast cascade above 2_1^+. The relatively large $2\rightarrow0$ energies in ^{74,76}Kr that make these nuclei look less deformed in their ground states than they really are, arise from an interaction between the 0_1^+ deformed and 0_2^+ near-spherical states that pushes down the 0_1^+ energy.[24] The 2^+ spherical state is quite high in energy, so there will be little mixing of the 2^+ and higher spin states, since the energies for the spherical structure grow much faster with spin than in the deformed band. In ^{72,74}Se, there also is considerable mixing of the deformed and spherical configurations near the band crossing at $I\simeq2-4$ in contrast to the situation in ^{74,76}Kr.

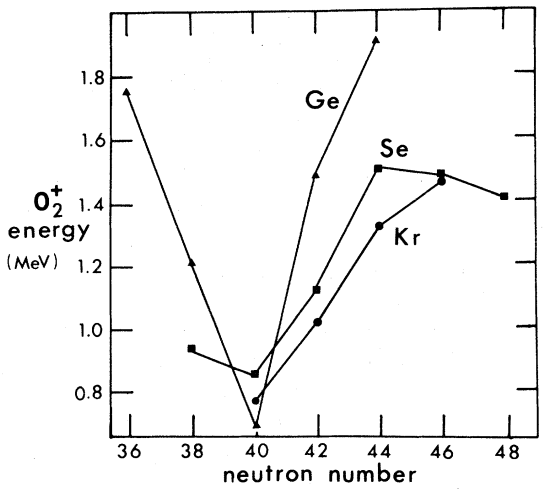

FIG. 9. The energies of the 0_2^+ levels as a function of neutron number for Ge, Se, and Kr isotopes.

In ^{74,76}Kr, we have a reversal in the shape coex-

istence from that in ^{72,74}Se with the ground states deformed and the excited 0_2^+ band near spherical. The origin and delicate balance of these two competing configurations can be understood in terms of the role of the proton number.[24] The magnitude of the deformation is surprising. The unperturbed $2_1^+ \rightarrow 0_1^+$ energy is calculated to be 237 keV. When scaled by $A^{5/3}$, this corresponds to a 35-keV first excited state for strongly deformed ^{240}Pu which has a 43 keV $2^+ \rightarrow 0^+$ energy.

The transition strengths in the ground-state band (Table IV) show that ^{76}Kr exhibits the strongest collective $B(E2)$'s known among nuclei in this mass region. These large $B(E2)$'s are consistent with the strong deformation discussed above for ^{76}Kr. The $B(E2)$ strengths of the ground-state band are, within the experimental error, consistent with those expected for a rotational nucleus. These, clearly, are not in line with a pure vibrational model.

The measured mean lives of the negative parity band levels lead to exceptionally large $B(E2)$ values for the (11^-)-9^-, 9^-- 7^-, and 7^--5^- transitions. The origin of such large $B(E2)$ strengths is not understood. The lifetime of the (13^-) state is a composite lifetime.

For the γ-type vibrational band, only composite lifetimes could be obtained. Even when using the composite lifetimes, which are undoubtedly larger than those of the levels, these levels exhibit large collectivity strength. Their collectivity is in agreement with that found for such levels in other nearby nuclei.[1] The presence of the γ vibrational levels also underscores the importance of strong deformation in these nuclei. The details of two-quasiparticle-plus-rotor calculations for all the even-A Kr isotopes are discussed in a following paper.[25]

The research at Vanderbilt University was supported by the U. S. Department of Energy under Contract No. DE-AS0534-ER0534, and at Oak Ridge National Laboratory through Contract No. W-7405-eng-26 with Union Carbide Corporation.

[1]J. H. Hamilton, R. L. Robinson, A. V. Ramayya, *Nuclear Interactions,* edited by B. A. Robson (Springer, New York, 1979), p. 253.

[2]M. Vergnes, *Structure of Medium-heavy Nuclei, 1979,* edited by G. S. Anagnostatos, C. A. Kalfas, S. Kossionides, T. Paradelis, L. D. Skouras, and G. Vourvopoulos (The Institute of Physics, Bristol, 1979), p. 25.

[3]U. Kaup, A. Gelberg, W. Gast, and P. von Brentano, *Structure of Medium-Heavy Nuclei* (Institute of Physics, London, 1980), p. 230.

[4]A. P. de Lima, A. V. Ramayya, J. H. Hamilton, B. Van Nooijen, R. M. Ronningen, H. Kawakami, R. B. Piercey, E. de Lima, R. L. Robinson, H. J. Kim, L. K. Peker, F. A. Rickey, R. Popli, A. J. Caffey, and J. C. Wells, Phys. Rev. C 23, 213 (1981).

[5]R. B. Piercey, J. H. Hamilton, and A. V. Ramayya, *Proceedings of the International School Nuclear Physics, Neutron Physics and Nuclear Energy* (Bulgarian Academy of Sciences, Varna, 1979), p. 449.

[6]J. Roth, L. Cleemann, J. Eberth, T. Heck, W. Neumann, M. Nolte, R. B. Piercey, A. V. Ramayya, and J. H. Hamilton, 4th International Conference on Nuclei Far From Stability, CERN Report CERN 81-09, 1981, p. 680.

[7]J. H. Hamilton, R. B. Piercey, R. Soundranayagam, A. V. Ramayya, C. F. Maguire, X. J. Sun, Z. Z. Zhao, J. Roth, L. Cleemann, J. Eberth, T. Heck, W. Neumann, M. Nolte, R. L. Robinson, H. J. Kim, S. Frauendorf, J. Döring, L. Funke, G. Winter, J. C. Wells, J. Lin, A. C. Rester, and H. C. Carter, *4th International Conference on Nuclei Far From Stability,* CERN Report 81-09, 1981, p. 391.

[8]R. B. Piercey, A. V. Ramayya, R. M. Ronningen, J. H. Hamilton, V. Maruhn-Rezwani, R. L. Robinson, and H. J. Kim, Phys. Rev. C 19, 1344 (1979).

[9]E. Nolte, Y. Shida, W. Kutschera, R. Prestele, and H. Morinaga, Z. Phys. 268, 267 (1974).

[10]J. Lin, A. C. Rester, J. C. Wells, H. K. Carter, R. B. Piercey, A. V. Ramayya, J. H. Hamilton, R. L. Robinson, and H. J. Kim, Bull. Am. Phys. Soc. 23, 574 (1978).

[11]L. C. Biedenharn and M. E. Rose, Rev. Mod. Phys. 25, 729 (1953).

[12]K. S. Krane, R. M. Steffen, and R. M. Wheeler, Nucl. Data Tables 11, 351 (1973).

[13]W. T. Milner *et al.*, DOPCO Vanderbilt University Computer Library Code.

[14]Z. Z. Zhao, Z. J. Sun, R. B. Piercey, J. H. Hamilton, C. F. Maguire, A. V. Ramayya, R. L. Robinson, H. J. Kim, and J. C. Wells, Chin. J. Nucl. Phys. (to be published).

[15]S. Kalbitzer, H. Oetzmann, H. Grahmann, and A. Feuerstein, Z. Phys. A 278, 223 (1976).

[16]L. C. Northcliff and R. F. Schilling, Nucl. Data Tables 7, 3 (1970).

[17]J. F. Ziegler and W. K. Chu, At. Nucl. Data 13, 463 (1979).

[18]D. Ward, J. S. Forster, H. R. Andrews, I.L.V. Mitchell, G. C. Ball, W. G. Davies, and G. I. Costa, Atomic Energy of Canada Limited Report AECL 5313, 1976.

[19]A. E. Blaugrund, Nucl. Phys. 88, 501 (1966).

[20]R. L. Robinson, H. J. Kim, R. O. Sayer, W. T. Milner, R. B. Piercey, J. H. Hamilton, A. V. Ramayya, J. C. Wells, and A. J. Caffrey, Phys. Rev. C 21, 613 (1980).

[21]D. L. Sastry, A. Ahmed, A. V. Ramayya, R. B. Piercey, H. Kawakami, R. Soundranayagam, J. H. Hamilton, C. F. Maguire, A. P. de Lima, S. Ramavataram, R. L. Robinson, H. J. Kim, and J. C. Wells, Phys. Rev. C 23, 2086 (1981).

[22]A. V. Ramayya, R. M. Ronningen, J. H. Hamilton, W. T. Pinkston, G. Garcia-Bermudez, R. L. Robinson, H. J. Kim, H. K. Carter, and W. E. Collins, Phys. Rev. C 12, 1360 (1975).

[23]R. M. Ronningen, A. V. Ramayya, J. H. Hamilton, W. Lourens, J. Lange, H. K. Carter, and R. O. Sayer, Nucl. Phys. A261, 439 (1976).

[24]R. B. Piercey, J. H. Hamilton, R. Soundranayagam, A. V. Ramayya, C. F. Maguire, X. J. Sun, Z. Z. Zhao, R. L. Robinson, H. J. Kim, S. Frauendorf, J. Döring, L. Funke, G. Winter, J. Roth, L. Cleemann, J. Eberth, W. Neumann, J. C. Wells, L. Lin, A. C. Rester, and H. K. Carter, Phys. Rev. Lett. 47, 1514 (1981).

[25]R. Soundranayagam, S. Ramavataram, A. V. Ramayya, J. H. Hamilton, and R. L. Robinson, Phys. Rev. C (to be published).